SODIUM LIDAR SYSTEM FOR OBSERVING ANTARCTIC MESOPAUSE TEMPERATURE OVER SYOWA STATION

Takuya D. KAWAHARA, Tsukasa KITAHARA, Fumitoshi KOBAYASHI, Yasunori SAITO and Akio NOMURA

Department of Information Engineering, Shinshu University, 500 Wakasato, Nagano 380-8553

Abstract: A new sodium lidar will be installed at Syowa Station ($69°00'$S, $39°35'$E) from 1999 to 2001 for the observation campaign of the Antarctic mesopause region. In the campaign the lidar is operated with HF and MF radars, a Fabry-Perot Doppler imager and several other auroral imagers. This is the first lidar measurement of the mesopause temperature in Antarctica and it will reveal the characteristics of gravity wave activities and the energetic interaction between the lower thermosphere and the upper mesosphere through the mesopause region over Antarctica.

For the temperature observations, a new laser transmitter is developed using injection-seeded Nd: YAG lasers. The principal advantage of this instrument is that the transmitter is simple and a reliable solid state system which requires less maintenance compared with ordinary dye laser type transmitters. This allows us to construct and operate it easily in Antarctica. As a result of sum frequency of seeded 1064 nm and 1319 nm laser pulses, narrow-band pulsed laser tuned to sodium D_2 line (589.1583 nm) is effectively emitted with a linewidth of below 0.1 pm. To eliminate temperature errors caused by sodium density variations, an AO frequency shifter is adopted to shift frequencies within sodium D_2 spectrum on a pulse to pulse basis. For daytime observations, an extreme narrowband (FWHM = 0.002 nm) Faraday filter is employed in the receiving system to reject sky background light. The estimated spatial resolution, temporal resolution and temperature accuracy of this system are 200 m, < 5 K and 10 min, respectively.

1. Introduction

The dynamics and chemistry of the mesosphere and the lower thermosphere (MLT) region are complex, and much attention has been paid. The MLT is energetically an important transition region between the lower and upper atmosphere. Atmospheric waves such as gravity wave, tide and planetary wave play an important role in this region in the transport of energy and momentum, and maintain the general circulation. In recent years, our understanding of this region has significantly been improved with the development of new techniques such as a sodium lidar or several kinds of radars. In particular, a sodium temperature lidar is one of the most powerful technique to probe absolute temperature profile in the mesopause region with an accuracy of 5 K, and with a temporal and height resolution of a few minutes and about 200 m, respectively. The first contribution of the temperature lidar measurements was the discovery of double temperature minimum structure at mesopause altitude (NEUBER *et al.*, 1988). Later, SHE *et al.* (1993) reported seasonal variation in the temperature measured with the lidar at Fort Collins, CO ($40.6°$N, $105°$W). The data clearly revealed that the mesopause altitude is comparatively high in winter ($\sim$190 K at 100 km

altitude) and low in summer ($\sim$178 K at 86 km altitude). They suggested that waves are possibly the main source to affect this region and cause the temperature variations. In polar regions, in addition to wave energy transports, high altitude magnetic field lines provide routes for solar wind particles to reach the middle atmosphere, where they interact with the neutral gas (RÖTTGER, 1991). Such an interaction, which is mainly associated with auroral disturbances, may cause some short-period variations of wind and temperature during geomagnetically active conditions. The energy injection of solar origin in to the earth atmosphere is also believed to be vital to our understanding of the processes for natural climate change. Another paper reports that a recent apparent increase in the occurrence of noctilucent clouds (NLCs) in the polar regions during summer is believed to be associated with decreasing mesopause temperatures, and the NLCs increased possibly oxidation of the greenhouse gas methane (GADSDEN, 1990; THOMAS et al., 1989). We think that it is rather crucial to probe temperature and its short and long period variation for better understanding of dynamical and chemical processes at polar mesopause altitude. However, the temperature observations have been limited so far in northern mid-latitudes, for example by the groups of Colorado State University or University of Illinois, or by University of Bonn group in northern high latitude at 69°N. Though VON ZAHN et al. (1996) performed a ship-borne observation in the southern hemisphere with a potassium temperature lidar between 71°S and 54°N, there has been no observation in Antarctica. Further the summertime antarctic temperature observations have never been made before, and seasonal variation of the temperature is unknown. With these backgrounds, we constructed a sodium temperature lidar system for the observation at Syowa Station, Antarctica. Using an ultra narrowband filter, the first summertime temperature observation in Antarctica will also be performed. With simultaneous wind field observation of MF radar (TSUTSUMI et al., 1997), seasonal variation in antarctic wind and temperature will provide important information about the Antarctic mesopause region.

Several groups have recently conducted mesospheric temperature measurements with the sodium temperature lidar. Based on an excimer-pumped dye laser system, University of Bonn group has developed the first sodium temperature lidar (FRICKE and VON ZAHN, 1985). They conducted several important studies of the mesopause thermal structure at Andøya, Norway (NEUBER et al., 1988; VON ZAHN and MEYER, 1989; LÜBKEN and VON ZAHN, 1989; KURZAWA and VON ZHAN, 1990; VON ZAHN, 1990; LÜBKEN and VON ZAHN, 1991). Later, Colorado State University and University of Illinois group developed more reliable system with a ring dye laser/pulsed dye amplifier technique (BILLS et al., 1991a; SHE et al., 1992). Since this system could produce reproducible frequency of individual laser pulse, they expanded their system not only to temperature measurement of the sodium layer but to Doppler wind measurement (SHE and YU, 1994; BILLS et al., 1991b). They also conducted several important studies at their observatory (SHE et al., 1993; BILLS and GARDNER, 1993). However, the disadvantage of the systems above is complexity and therefore the systems require careful and hard maintenance. Recently, JEYS et al. (1989) reported a new type of laser system based on Nd: YAG lasers, and based on the study of them, CHIU et al. (1994) completed a narrow band laser transmitter for the sodium D_2 transition wavelength. The sum frequency of two radiations of the Nd: YAG laser operating near 1064 nm and 1319 nm

produce 589 nm laser after they pass through a non-linear crystal such as lithium triborate (LBO). Because the system consists of all solid-state components, it is simple and requires less maintenance compared with ordinary transmitters. Other advantages of the system are the higher reliable peak power and better beam quality. We adopted this laser for our temperature lidar system. The system is relatively compact and therefore it can be transported easily even to Antarctica.

2. Temperature Measurement Technique

The two-frequency sodium lidar technique measuring mesospheric temperature is described in detail in FRICKE and VON ZAHN (1985) or BILLS et al. (1991a). The sodium D_2 Doppler-broadened fluorescence spectrum is plotted in Fig. 1a as a function of frequency for three temperatures (from BILLS et al., 1991a). The spectrum is originally composed of six hyperfine lines. Since the width of each Gaussian lineshape is proportional to the square root of temperature, the sum of these six Gaussian lineshapes contributes to the overall temperature dependence of the fluorescence spectrum. Because the D_{2a} peak and the intermediate minimum between the D_{2a} and D_{2b} peaks are particularly sensitive to temperature, the ratio of the minimum to the peak can be used to derive the sodium temperature accurately (Fig. 1b). By collecting lidar photocount profiles with a narrowband lidar at each of these two wavelengths, then taking the ratio of the photocounts collected at each altitude, one can derive the vertically resolved temperature structure throughout the sodium layer region.

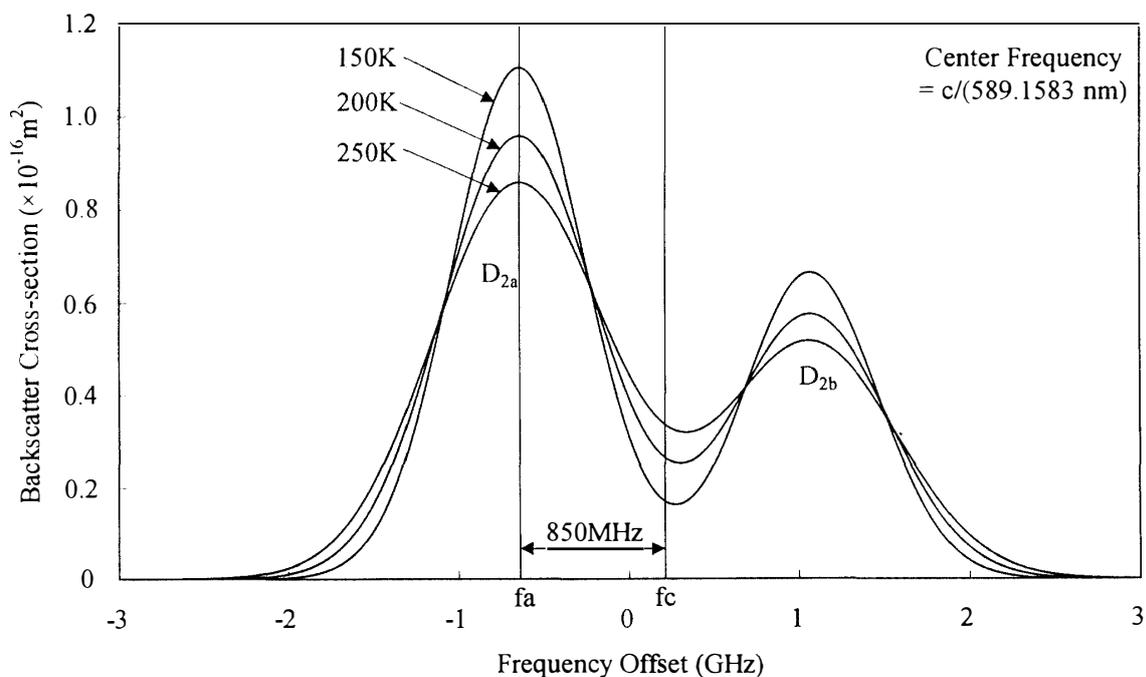For the laser frequency reference, a sodium vapor cell heated at about 50°C is used

Fig. 1a.   Sodium D_2 Doppler-broadened absorption spectrum plotted as a function of frequency for three temperatures. The D_{2a} and D_{2b} hyperfine line groups are depicted as well (from BILLS et al., 1991a).
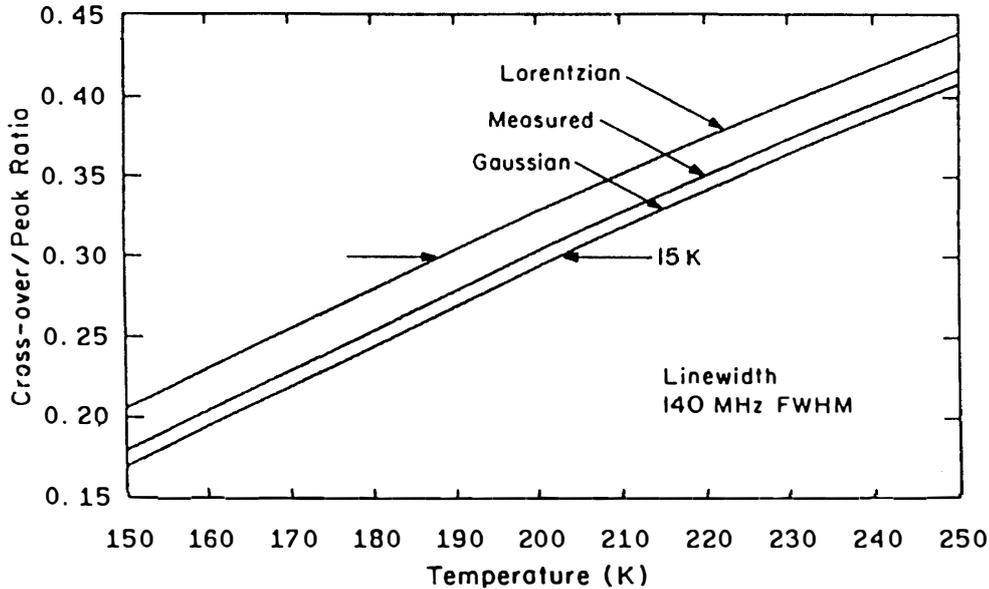
Fig. 1b.   Sodium crossover to D_{2a} peak resonance signal ratio vs temperature for three laser lineshapes with 140 MHz FWHM bandwidth: Lorentzian, Gaussian, and the lineshape measured by BILLS et al. (1991a).

to know the absolute frequencies. If a D_2 resonance laser goes through the sodium cell, one can measure the fluorescence light perpendicular to the laser line. BILLS et al. (1991 a) conducted a fluorescence signal measurement from the sodium cell with the 589 nm narrowband ($<$ 1 MHz RMS) cw ring laser. A mirror is used to retro-reflect the laser beam into the cell. Under simultaneous illumination of the two counterpropagating beams at a saturated intensity, the sodium fluorescence spectrum emitted by the cell exhibits Doppler-free features at the D_{2a} and D_{2b} peaks ($f_a = -648.8$ MHz and $f_b = 1066.9$ MHz, respectively) and at the crossover resonance ($f_c = 200.3$ MHz). Since f_a is at the D_{2a} peak and f_c is close to the minimum between the D_{2a} and D_{2b} peaks, the fluorescence signal level from the sodium layer at these two frequencies is relatively insensitive to small frequency errors in the laser. For this reason, we also choose f_a and f_c for our temperature measurement. The frequency switching method between these frequencies with an AO frequency shifter is described in the next section.

The number of photons scattered from the sodium layer over a vertical range interval is proportional to the convolution of the laser lineshape with the sodium D_2 Doppler-broadened fluorescence spectrum. BILLS et al. (1991a) pointed out that the temperature error is very sensitive to the laser lineshape. Therefore, knowledge of only the laser linewidth is insufficient for accurate temperature measurements. They compared the temperature between the measured lineshape and several kinds of assumed lineshapes such as Gaussian and Lorentzian with the same linewidth of 140 MHz FWHM. Each of these lineshapes can be convolved with the sodium D_2 fluorescence spectrum, and the ratio of the value at f_c to the value at f_a can be computed as a function of temperature. The temperature uncertainty was found to be as large as 15 K, due to lineshape uncertainty. Therefore the laser lineshape must be measured accurately, since the ratio-temperature curve is most sensitive to these lineshape features. The FWHM of our laser linewidth is expected to be less than 150 MHz which is narrower than the

spectral resolution of ordinary spectrum analyzers. We are planning to measure the lineshape in the same procedure found in the paper of SHE *et al.* (1992).

3. Sodium Temperature Lidar System

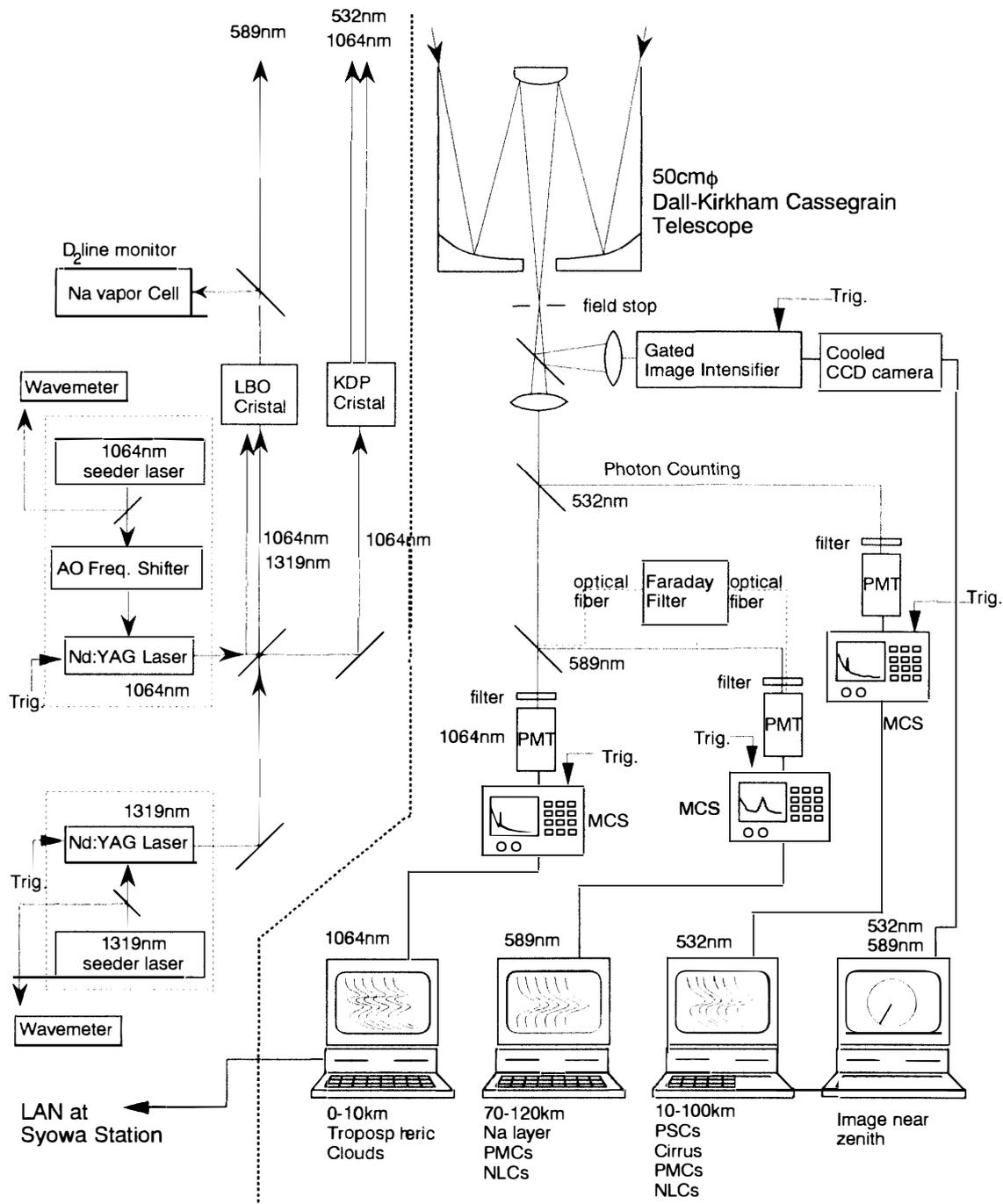One of the interesting coincidence of nature is that the sum frequency of two

Fig. 2. Schematic of the sodium temperature lidar system.

Table 1.   Specification of the sodium temperature lidar.

Transmitter	
Wavelength	589 nm, 532 nm, 1064 nm
Spectral width	< 100 MHz
Tuning range	± 2 GHz
Pulse energy	< 40 mJ (589 nm)
	< 50 mJ (532 nm, 1064 nm)
Repetition rate	10 Hz
Pulse width	> 30 ns
Beam divergence	< 0.2 mrad
Polarization	linear
Receiver	
Telescope	ϕ 0.5 m Dall-Kirkham Cassegrain
Aperture area	0.20 m²
F.O.V.	1–3 mrad
Interference filter	FWHM 1.0 ± 0.2 nm
Na Faraday filter	FWHM 2 pm, $T_{peak} = 12\%$
Temperature accuracy	~5 K
Height resolution	192 m (gate width 1.28 μs)
Temporal resolution	10 min

appropriately tuned Nd: YAG lasers near 1064 nm and 1319 nm can generate resonant wavelength of the sodium D_2 transition (589.1583 nm). JEYS et al. (1989) firstly demonstrated the possibility of the sodium layer measurement with the laser transmitter using this method. They tuned the sum radiation with an intra-cavity etalon over a 0.3 nm range, nearly centered at the sodium D_2 transition, easily encompassing the Doppler-broadened sodium absorption width of 0.003 nm. Since the sodium D_1 transition is nearly 0.6 nm apart from the sodium D_2 transition, there is no possibility to generate resonant radiation of the D_1 transition. Later CHIU et al. (1994) completed the transmitter with injection-seeded Nd:YAG lasers. The spectral linewidth was narrow, less than 100 MHz (0.1 pm), which is enough for the temperature observation of the sodium layer. Our transmitter follows Chiu's system and is constructed in HOYA Continuum, Inc.

Figure 2 shows an overall layout of the lidar system. The major system parameters are summarized in Table 1. Seed laser technique used in this system is quite useful because it makes the pulsed laser spectral width narrow (less than 150 MHz) without reducing the laser energy unlike etalons. The pulsed laser frequency is tuned by the frequency controller of the seed laser. In the measurement of sodium layer with this system, it takes rather long time, more than 10 s, to shift the frequency between f_a and f_c. Photocounts are acquired at one frequency for the duration of a few minutes followed by acquisition at the other frequency for another minutes. In this procedure, during the data acquisition at different excitation frequencies, atmospheric sodium density may change and temperature error results. To avoid this, an AO frequency shifter (N17425, Neos) is inserted between the laser line of the 1064 nm seed laser (Fig. 3). The seed
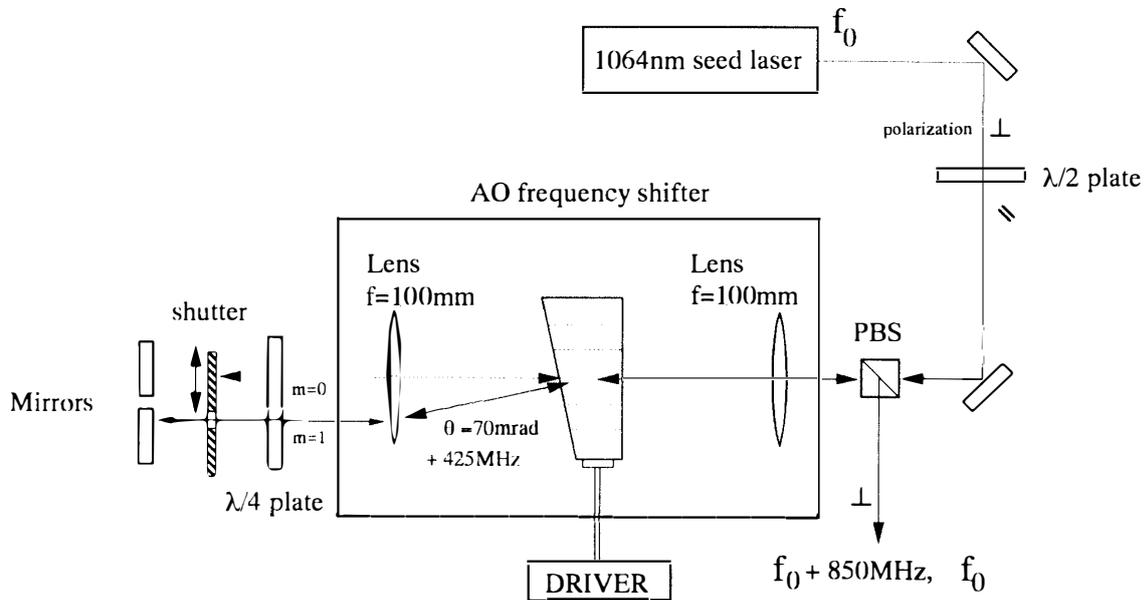
Fig. 3. Schematic of the AO frequency shifter. Solid line depicts the light pass of the shifted frequency.

laser frequencies are locked to produce the D_{2a} peak frequency (f_a) of the sodium D_2 transition, and by the frequency shifter the frequency is shifted to the other (f_c). The retro-reflected seed laser passes through a $+425$ MHz AO shifter again and the frequency is totally shifted by $+850$ MHz (from f_a to f_c). Because AO modulation response time is quite fast, the laser frequency can be shifted on a pulse to pulse basis and it eliminates errors caused by sodium density variations. Together with 589 nm, the transmitter also emits 1064 nm and 532 nm laser pulses for the observation of polar stratospheric clouds or cirrus. The 532 nm channel is used as a Rayleigh lidar to obtain temperature profiles between 35–60 km height.

Scattered light is collected by a 0.5 m diameter Dall-Kirkham Cassegrain telescope (Kiyohara Optical Lab.) by pulse to pulse shot. The light is focused through a field stop iris and collimated by a lens. After separated by dichroic mirrors, the light pass through an interference filter centered at the each laser wavelength and is photocounted by a cooled low-noise photomultiplier tube (R943-02 for 532 nm and 589 nm, R3236 for 1064 nm, Hamamatsu Photonics Co.). The PMT pulse current is processed to produce digital pulses corresponding to each photon received, and these pulses are counted over 96 m range intervals by Multichannel Scaler (SR430, Stanford Research Systems, Inc.). For the temperature measurement with the 589 nm channel, two scalers are independently used for the accumulation at the each frequency, f_a and f_c. The collected photocount data are transferred to a computer to display real-time A-scope and are used for further processing to derive the temperature. All the system is controlled by the personal computers through GPIB interface. The PMT is gain switched to prevent saturation of photocounts by the strong returns below 15 km. Further, to avoid the strong scattered light damaging the photoelectric surface of the PMT or inducing secondary electrons, the low altitude returns (< 10 km) is masked by an optical chopper. The chopper also gives laser trigger timing. A cooled CCD camera (CV-04, Mutoh)
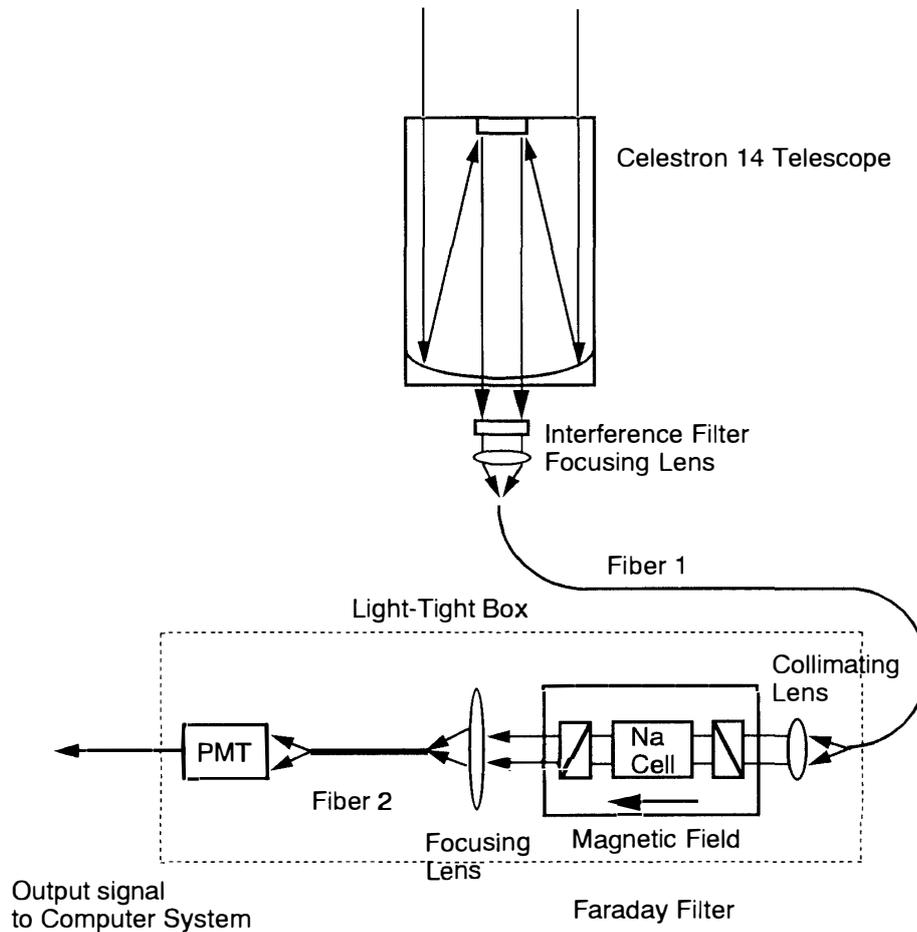
Fig. 4. Schematic of the Faraday receiver system with a fiber-coupled sodium vapor dispersive Faraday filter (from CHEN et al., 1996).

images zenith direction to align the axes of the telescope and the laser beams.

A fiber coupled dispersive sodium Faraday filter shown in Fig. 4 (from CHEN *et al.*, 1996) is installed for the daytime observation of mesospheric temperature. The FWHM transmission of the filter is quite narrow, 2 pm, which is comparable to the width of sodium D_2 resonance spectrum of 3 pm and the peak transmission is quite high, 86%. Sky background light is effectively rejected to 2×10^5. A Colorado State University group has already fabricated the Faraday filter and made successful wind/temperature observations in daytime and nighttime (CHEN *et al.*, 1993, 1996). The Faraday filter consists of a temperature controlled ($\sim 170°C$) sodium vapor cell ($\phi 25$ mm, $l = 25$ mm, Opthos Instruments, Inc.) between a pair of crossed polarizers (03PTH403/A, Melles Griot), and rare-earth magnets which make a strong axial magnetic field in the cell position. Because of Faraday rotation and Zeeman effect, near sodium resonance light is alternatively pass through the crossed polarizers. Since strong magnetic field of 1800 G may be achieved, the Faraday filter is connected with optical fiber cable and placed away from the PMT. The Faraday filter enables us to make winter and summer observations with HF and MF radars and is expected to reveal seasonal variations in mesospheric temperature and wind.

4. Conclusion

We presented in this paper the sodium temperature lidar system and the future lidar observation plan at Syowa Station, Antarctica. The daytime and nighttime temperature observations will be the first ever made of the mesopause region in Antarctica. The injection-seeded Nd: YAG laser base transmitter is newly developed for the sodium D_2 resonant wavelength. It is a reliable and easily operated system for the continuous observation. Moreover, the combined operation with MF and HF radars and other optical instruments at Syowa Station would provide us invaluable information about atmospheric dynamics in vertically and horizontally wide spatial area.

Acknowledgments

It is our great pleasure to thank Prof. C. S. GARDNER of University of Illinois and Prof. C. Y. SHE of Colorado State University for their useful comments. We also thank Mr. KATO in HOYA Continuum, Inc. for constructing the solid state laser system.

References

BILLS, R. E. and GARDNER, C. S. (1993): Lidar observations of the mesopause region temperature structure at Urbana. J. Geophys. Res., 98, 1011–1021.

BILLS, R. E., GARDNER, C. S. and SHE, C. Y. (1991a): Narrowband lidar technique for sodium temperature and Doppler wind observations of the upper atmosphere. Opt. Eng., 30, 13–21.

BILLS, R. E., GARDNER, C. S. and FRANKE, S. J. (1991b): Na Doppler/temperature lidar: Initial mesopause region observations and comparison with the Urbana Medium Frequency radar. J. Geophys. Res., 96, 22701–22707.

CHEN, H., SHE, C. Y., SEARCY, P. and KOREVAAR, E. (1993): Sodium-vapor dispersive Faraday filter. Opt. Lett., 18, 1019–1021.

CHEN, H., WHITE, M. A., KRUEGER, D. A. and SHE, C. Y. (1996): Daytime mesopause temperature measurements with a sodium-vapor dispersive Faraday filter in a lidar receiver. Opt. Lett., 21, 1093–1095.

CHIU, P. H., MAGANA, A. and DAVIS, J. (1994): All solid-state single-mode sum frequency generation of sodium resonance radiation. Adv. Solid-State Lasers, 20, 367–371.

FRICKE, K. H. and VON ZAHN, U. (1985): Mesopause temperatures derived from probing the hyperfine structure of the D_2 resonance line of sodium by lidar. J. Atmos. Terr. Phys., 47, 499–512.

GADSEN, M. (1990): A secular change in noctilucent cloud occurrence. J. Atmos. Terr. Phys., 52, 247–251.

JEYS, T. H., BRAILOVE, A. A. and MOORADIAN, A. (1989): Sum frequency generation of sodium resonance radiation. Appl. Opt., 28, 2588–2591.

KURZAWA, H. and VON ZAHN, U. (1990): Sodium density and atmospheric temperature in the mesopause region in polar summer. J. Atmos. Terr. Phys., 52, 981–993.

LÜBKEN, F.-J. and VON ZAHN, U. (1989): Simultaneous temperature measurements in the mesosphere and lower thermosphere during the MAC/EPSILON campaign. Planet. Space Sci., 37, 1303–1314.

LÜBKEN, F.-J. and VON ZAHN, U. (1991): Thermal structure of the mesopause region at polar latitudes. J. Geophys. Res., 96, 20841–20857.

NEUBER, R., VON DER GATHEN, P. and VON ZAHN, U. (1988): Altitude and temperature of the mesopause at 69°N latitude in winter. J. Geophys. Res., 93, 11093–11101.

RÖTTGER, J. (1991): MST radar and incoherent scatter contributions to studying the middle atmosphere. J. Geomagn. Geoelectr., 43, Suppl., 563–596.

SHE, C. Y. and YU, J. R. (1994): Simultaneous three-frequency Na lidar measurements of radial wind and temperature in the mesopause region. Geophys. Res. Lett., **21**, 1771–1774.

SHE, C. Y., YU, J. R., LATIFI, H. and BILLS, R. E. (1992): High-spectral-resolution fluorescence light detection and ranging for mesospheric sodium temperature measurements. Appl. Opt., **31**, 2095–2106.

SHE, C. Y., YU, J. R. and CHEN, H. (1993): Observed thermal structure of a midlatitude mesopause. Geophys. Res. Lett., **20**, 567–570.

THOMAS, G. E., OLIVERO, J. J., JENSEN, E. J., SCHROEDER, W. and TOON, O. B. (1989): Relation between increasing methane and the presence of ice clouds at the mesopause. Nature, **338**, 490–492.

TSUTSUMI, M., EJIRI, M., OKANO, S., SATO, N., YAMAGISHI, H., IGARASHI, K. and TSUDA, T. (1997): MF radar observations of Antarctic mesosphere and lower thermosphere. Proc. NIPR Symp. Upper Atmos. Phys., **10**, 109–116.

VON ZAHN, U. (1990): Temperature and altitude of the polar mesopause in summer. Adv. Space Res., **10**, (12)223–(12)231.

VON ZAHN, U. and MEYER, W. (1989): Mesopause temperature in polar summer. J. Geophys. Res., **94**, 14647–14651.

VON ZAHN, U., HÖFFNER, J., ESKA, V. and ALPERS, M. (1996): The mesopause altitude: only two distinctive levels worldwide? Geophys. Res. Lett., **23**, 3231–3234.